ELSEVIER

Polymer Vol. 37 No. 3, pp. 485–492, 1996

0032-3861/96/$15.00 + 0.00

The deduction of fine structural details of gas separation hollow fibre membranes using resistance modelling of gas permeation

S. J. Shilton* and G. Bell
Department of Chemical and Process Engineering, University of Strathclyde, James Weir Building, 75 Montrose Street, Glasgow G1 1XJ, UK

and J. Ferguson
Department of Pure and Applied Chemistry, University of Strathclyde, Thomas Graham Building, 295 Cathedral Street, Glasgow G1 1XL, UK
(Received 1 December 1994; revised 1 May 1995)

Gas transfer through asymmetric polysulfone hollow fibre membranes has been modelled, allowing fine details of fibre structure to be deduced from gas permeation characteristics. The structural information is used to interpret the relationship between spinning conditions and fibre properties. Dope concentration determines the general morphology of the fibre, such as the porosity (voidage fraction), thickness of the active layer and order of magnitude of surface porosity (fraction of surface area that is pores), and thus it sets the permeability and level of selectivity that are likely to be achieved on coating. The selectivity of the solid polymer (the maximum selectivity achievable by any membrane if coating is highly effective or if no surface pores are present) was found to increase with increasing dope extrusion rate. The elevated levels of shear in the spinneret may enhance the orientation of polymer molecules. Increasing the jet stretch ratio during spinning had a detrimental effect on solid polymer selectivity. Increased elongational strain possibly results in an unfavourable polymer structure.

(Keywords: gas separation; hollow fibre membranes; spinning conditions)

INTRODUCTION

Little has been published on the effect of spinning conditions on the performance of gas separation hollow fibre membranes. Work that has been reported focuses on coagulation conditions during spinning[1], and any effects on gas permeation are limited to an empirical description owing to the complexity of the polymer precipitation process.

The effect of spinning rheology on the performance of gas separation hollow fibre membranes has been investigated[2,3] with a view to improving fundamental knowledge. The rate of shear experienced in the spinneret and the amount of elongation undergone by the extruded filament were found to have an effect on the gas permeation performance of the hollow fibre membranes.

In the current paper, gas transfer through asymmetric membranes is modelled in order to elucidate the relationship between spinning conditions and membrane performance. The modelling allows fine details of fibre structure, such as the thickness of the active layer, surface porosity and solid polymer selectivity, to be deduced from gas permeation data. The structural information is then used to interpret the relationship between rheological conditions during spinning and membrane performance.

The principles of applying flow resistances in series and parallel in order to describe gas permeation through asymmetric membranes were first outlined by Henis and Tripodi[4,5], who predicted that a membrane useless for gas separation owing to the presence of surface pores or imperfections could exhibit gas separation properties akin to the capabilities of the solid polymer once coated with silicone. They applied the resistance approach to typical membrane structures and made assumptions as to the nature of the deposition of the coating material (e.g. the thickness of the silicone layer and pore penetration depth). The performance of these hypothetical coated membranes was predicted using their model.

Fouda *et al.*[6] exposed limitations in the Henis and Tripodi model when fitting actual gas permeation results to possible membrane structures. They then introduced the Wheatstone bridge model which better explained the permeation data. In the current paper, the resistance model approach is applied to the uncoated and coated permeation properties of laboratory-produced hollow fibres[2,3] in order to deduce details of their structure.

*To whom correspondence should be addressed

THEORY

Pore size and flow mechanisms

Gas transfer through membranes is governed by three major flow mechanisms (all parameters are defined in the Appendix).

1. Solution diffusion. This occurs when the membrane is completely non-porous. Gas transfer is controlled by the permeation properties of the solid polymer

$$Q = \frac{DS}{L} A\Delta p = \frac{\bar{P}}{L} A\Delta p \tag{1}$$

2. Knudsen diffusion. This type of flow occurs[7] when the Knudsen number λ/r is greater than 10. For Knudsen diffusion[8,9]

$$Q = \frac{8}{3}\left(\frac{1}{2\pi R_0 TM}\right)^{\frac{1}{2}} \frac{r}{L} A_P A\Delta p \tag{2}$$

3. Viscous flow. This occurs[7] when the Knudsen number λ/r is less than 0.01. For viscous flow[8]

$$Q = \frac{r^2}{8R_0 T}\frac{1}{L\eta}\left(\frac{p_f + p_p}{2}\right) A_P A\Delta p \tag{3}$$

The viscosity (η) of a gas is essentially independent of pressure. It can be shown from kinetic theory that

$$\eta = \left(\frac{MR_0 T}{\pi^3}\right)^{\frac{1}{2}} \frac{1}{Nd_m^2} \tag{4}$$

Also from kinetic theory, the mean free path of a gas molecule is given by

$$\lambda = \frac{R_0 T}{2^{\frac{1}{2}}\pi p N d_m^2} \tag{5}$$

Important properties of the gases and polymers studied are included in *Tables 1* and *2*. Values of viscosity were taken from the literature and molecular diameters evaluated from equation (4). Mean free paths were calculated from equation (5).

Between the extremes of Knudsen diffusion and viscous flow, i.e. when $10 > \lambda/r > 0.01$, there lies the complex transition region where the flow changes character progressively from Knudsen to viscous. Flow in this region has been described by Present and de Béthune[12]. According to Dushman[13], even when $\lambda/r = 1$, 85% of the total flow occurs by Knudsen diffusion. The mean free path λ depends on the molecular diameter d_m, which in turn depends on the physical property used in its determination. The values in *Table 1* originate from gas viscosities, but had they been based on the van der Waals co-volume the mean free paths would have almost doubled[14,15]. The mean free path varies inversely with pressure. For the purposes of predicting pore sizes and flow regimes it would seem most appropriate to base λ on the mean pressure in the membrane, typically 3.5 bar (1 bar = 100000 Pa) in this work. This reduces λ values based at 1 atm (1 atm = 101325 Pa) by a factor of 3.5. All things considered, the pore sizes corresponding to the different flow regimes in *Table 3* are estimated from the Knudsen number conditions.

From equations (2)–(4), the ratio of flows based on Knudsen diffusion and viscous flow for a particular pore size is given by

$$\frac{Q_{\text{viscous}}}{Q_{\text{Knudsen}}} = \frac{2^{\frac{1}{2}}3\pi^2 N d_m^2 p_{\text{mean}}}{64 R_0 T} r \tag{6}$$

Under the conditions of the present work, equation (6) reduces to

$$\frac{Q_{\text{viscous}}}{Q_{\text{Knudsen}}} = 0.001r \tag{7}$$

where r is in angstroms.

Table 1 Physical properties of CO_2 and CH_4

Gas	Molecular weight M ($g\,mol^{-1}$)	Viscosity η at 25°C ($N\,s\,m^{-2}$)	Molecular diameter d_m (Å)	Mean free path λ at 25°C and 1 atm (Å)
CO_2	44	15	4.6	446
CH_4	16	11	4.1	551

Table 2 Intrinsic gas permeation properties of polysulfone and dimethylsilicone

Polymer	$10^9\ \bar{P}_{CO_2}$ (cm^3 (STP) cm s^{-1} cm^{-2} $cmHg^{-1}$)	$10^9\ \bar{P}_{CH_4}$ (cm^3 (STP) cm s^{-1} cm^{-2} $cmHg^{-1}$)	$\Omega_{CH_4}^{CO_2}$
Polysulfone	0.45[a]	0.016	28[a]
Dimethylsilicone	325[b]	95[b]	3.4

[a] From Chern *et al.*[10]
[b] From Robb[11]

Table 3 Pore size correspondence to flow regime

Pore radius r (Å)[a]	Flow regime
Non-porous	Solution diffusion
< 30	Knudsen diffusion
= 300	85% Knudsen diffusion
> 30000	Viscous flow

[a] 1 Å = 0.1 nm

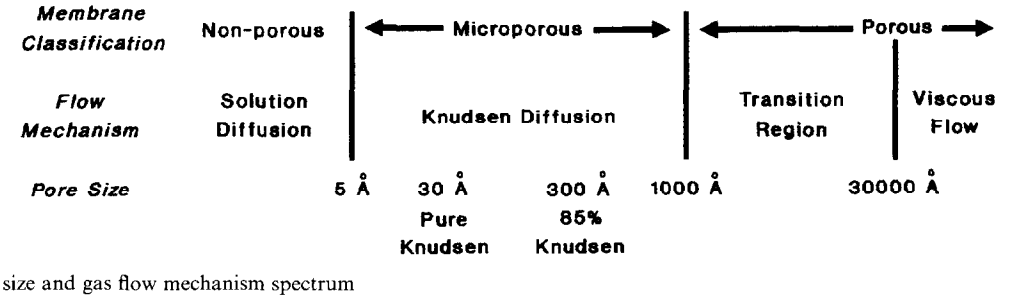

Figure 1 Pore size and gas flow mechanism spectrum

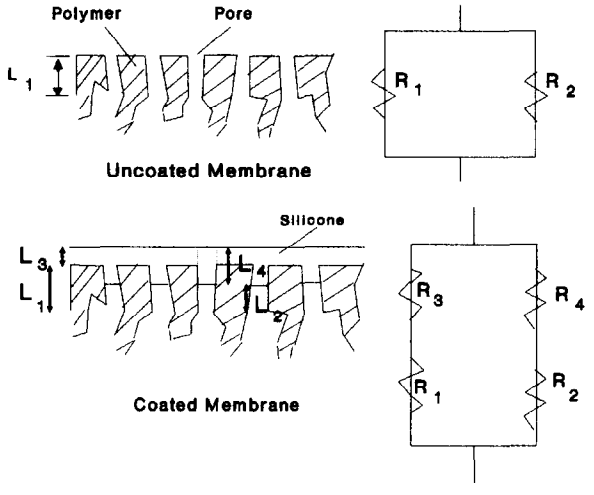

Figure 2 Resistance modelling: gas transfer through asymmetric membranes

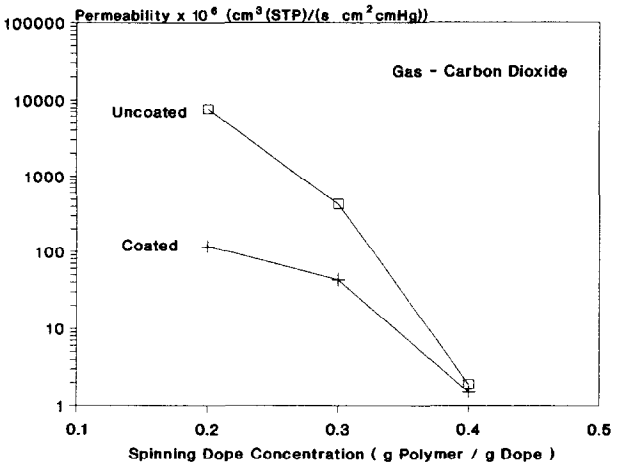

Figure 3 Effect of dope concentration on permeability

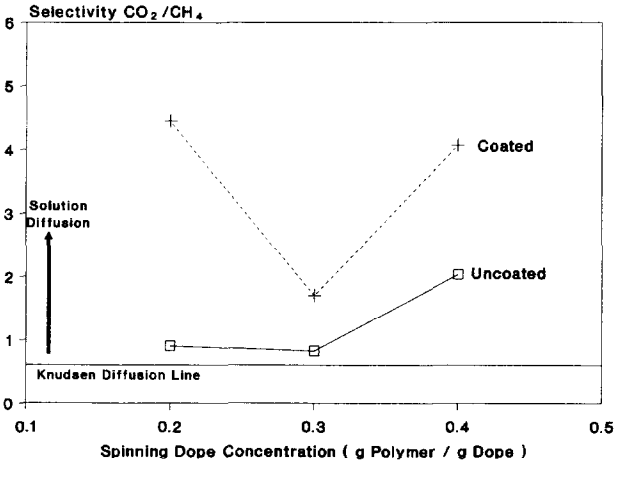

Figure 4 Effect of dope concentration on selectivity

Equation (7) shows that at a pore radius of 1000 Å, gas flow rates based on Knudsen diffusion and viscous flow are equal. Electron micrographs[2] have revealed no pores in the fibres at magnifications of up to 10 000. This suggests that generally the membranes have pore sizes of less than 100 Å, and thus pore flow can be assumed to be exclusively Knudsen. *Figure 1* summarizes the complete pore size and flow mechanism spectrum.

Resistance modelling of gas permeation

The permeation of a gas through a membrane can be described by the general equation

$$Q = PA\Delta p \tag{8}$$

The flow mechanisms discussed in the previous section can be represented by permeability expressions

$$P_{\text{solution diffusion}} = \frac{\bar{P}}{L} \tag{9}$$

$$P_{\text{Knudsen diffusion}} = \frac{8}{3}\left(\frac{1}{2\pi R_0 TM}\right)^{\frac{1}{2}}\frac{r}{L}A_P \tag{10}$$

$$P_{\text{viscous flow}} = \frac{r^2}{8R_0T}\frac{1}{L\eta}p_{\text{mean}}A_P \tag{11}$$

The resistance to permeation R can be defined as

$$R = \frac{1}{PA} \tag{12}$$

The resistance model used to depict fibre structure and gas permeation is shown in *Figure 2*. The resistance arrangement is the basic form of the Fouda *et al.*[6] model, but includes silicone penetration into the active layer pores. Another departure from the Fouda *et al.* model is the explicit use of the Knudsen permeability expression in the resistance equations, thus allowing the calculation of pore radius.

The following equations represent the resistance network and are applied to actual permeation data.

$$RU_iPU_iA = 1 \tag{13}$$

$$RC_iPC_iA = 1 \tag{14}$$

$$RU_i(R1_i + R2_i) = R1_iR2_i \tag{15}$$

$$\Omega URU_i(\Omega_1 R1_i + \Omega_2 R2_i) = \Omega_1 R1_i \Omega_2 R2_i \tag{16}$$

$$RC_i(R1_i + R4_i + R2_i) = R1_i(R4_i + R2_i) \tag{17}$$

$$\Omega CRC_i(\Omega_1 R1_i + \Omega_4 R4_i + \Omega_2 R2_i) = \Omega_1 R1_i(\Omega_4 R4_i + \Omega_2 R2_i) \tag{18}$$

$$R1_i\bar{P}_{pi}A = L_1 \tag{19}$$

$$R4_i\bar{P}_{Ci}A_PA = L_4 \tag{20}$$

$$R2_irA_PA = \frac{3}{8}(2\pi R_0TM)^{\frac{1}{2}}L_1 \tag{21}$$

When using the resistance model with the experimental data, a number of simplifications become apparent and are implicit in the above equations. The simplifications are as follows.

1. A_P is much smaller than 1, so the area of the solid polymer equals the membrane area A.
2. L_4 is much smaller than L_1, so on coating, the length L_2 of the open pore for Knudsen diffusion equals L_1.
3. On coating, the resistance offered by the outer silicone layer ($R3$) is negligible. (Even for the most permeable

Table 4 Effect of dope concentration on fibre structure[a]

Dope concentration (% w/w)	Thickness of active layer (Å)	Surface porosity	Pore radius (I) (Å)	Pore number (I) (cm^{-2})	Distance between pores (I) (Å)	Pore radius (II) (Å)	Pore number (II) (cm^{-2})	Distance between pores (II) (Å)
20	0.14×10^4	148×10^{-6}	100.0	43.1×10^6	1.52×10^4	1000	3.87×10^4	50.8×10^4
30	3.00×10^4	136×10^{-6}	75.5	62.2×10^6	1.27×10^4	1000	7.84×10^4	35.7×10^4
40	4.31×10^4	1.25×10^{-6}	38.0	2.76×10^6	6.02×10^4			

[a] The dope was polysulfone in dimethylformamide. The intrinsic selectivity of polysulfone for CO_2 over CH_4 was assumed constant at 28. On coating, the L_4/r ratio was 0.521. Gas transport was by solution diffusion and Knudsen diffusion

Table 5 Effect of dope extrusion rate on gas permeation properties[a]

	Run 1	Run 2	Run 3
DER ($cm^3 min^{-1}$)	0.7–1.0	1.0–1.5	1.5–2.0
Uncoated 10^4 P (cm^3 (STP) s^{-1} cm^{-2} $cmHg^{-1}$)	0.0097–0.0140	0.0161–0.0383	0.0141–0.0605
Coated 10^4 P (cm^3 (STP) s^{-1} cm^{-2} $cmHg^{-1}$)	0.0077–0.0172	0.0121–0.0244	0.0094–0.0144
Uncoated Ω	3.03–1.75	1.82–2.23	1.92–0.87
Coated Ω	3.50–4.65	3.36–5.32	3.84–4.06

[a] The dope was 40% w/w polysulfone in dimethylformamide and the JS was constant at 1. The permeabilities refer to CO_2 and the selectivities are for CO_2 over CH_4

Table 6 Effect of jet stretch on gas permeation properties[a]

	Run 1
JS	0.7–1.0–1.5
Uncoated 10^4 P (cm^3 (STP) s^{-1} cm^{-2} $cmHg^{-1}$)	0.0167–0.0140–0.0352
Coated 10^4 P (cm^3 (STP) s^{-1} cm^{-2} $cmHg^{-1}$)	0.0156–0.0172–0.0193
Uncoated Ω	2.42–1.75–0.90
Coated Ω	5.03–4.65–3.11

[a] The dope was 40% w/w polysulfone in dimethylformamide and the DER was constant at 1 cm^3 min^{-1}. The permeabilities refer to CO_2 and the selectivities are for CO_2 over CH_4

coated fibres, a silicone layer 1 μm thick is required to exert just 10% of the overall resistance. Electron microscopy of fibre cross-sections could not detect the presence of the outer silicone layer at magnifications of up to 10 000 in any of the fibres, showing that the coating thickness is in fact much smaller than 1 μm and hence exerts negligible resistance.)

The model equations were solved by computer using measured uncoated and coated hollow fibre permeabilities for CO_2 and CH_4. The equation-solving software package 'TK Solver Plus' (Universal Technical Systems, Rockford, IL, 1987) was used.

RESISTANCE MODEL RESULTS: EFFECT OF SPINNING CONDITIONS ON FIBRE STRUCTURE AND PERFORMANCE

Introduction

Figures 3 and *4* show the influence of dope concentration on hollow fibre permeability and selectivity[3]. These data were fed into the resistance model equations to deduce the fine structural details of the membranes. The results are shown in *Table 4*.

Tables 5 and *6* show the influence of dope extrusion rate (DER) and jet stretch (JS) on hollow fibre permeability and selectivity[3]. These permeation results are more sensitive than those relating to dope concentration. Gas permeation performance is subject to the slightest alterations in the character of the surface pores. The delicate nature of the membrane surface also results in susceptibility to random pinholes or imperfections. Thus, subtle alterations in process conditions, practical procedures or handling in spinning, washing, drying, potting up, coating or gas permeation testing inevitably cause variations in the separation performance of the hollow fibres. As a result, a distinction has been made between spinning runs in order to confirm the direction of the trends involved.

In order to extract values to feed into the resistance model equations, an overall trend line was drawn through the DER and JS data sets (least squares regression). The overall trend data reasonably represent the nature of the rheological effects on the permeation properties of the hollow fibres. The overall trend data are given in *Tables 7* and *8* alongside the resulting fine structural details of the membranes deduced by the resistance model.

In the investigations of dope extrusion rate and jet stretch ratio (based on 40% w/w spun polysulfone hollow fibres), the thickness of the active layer was assumed constant. Active layer thickness is dependent on phase inversion effects and hence will alter with differing dope concentrations. However, DER and JS are subtle rheological parameters which have minimal influence on phase inversion and hence have negligible effects on active layer thickness. This is in accordance with electron microscope work where no distinction in structure, in particular active layer thickness, was detected between fibres within one dope concentration[2]. (This statement is based on magnifications of up to 4000 where the active layer could be clearly distinguished from the rest of the fibre cross-section.)

The literature polysulfone selectivity of 28 (CO_2 over CH_4)[10] was used to represent fibres spun at a DER of 1 cm^3 min^{-1} and a JS of 1. When investigating dope concentration, the polysulfone selectivity was assumed constant at 28.

Table 7 Overall permeation data and the effect of dope extrusion rate on fibre structure[a]

DER ($cm^3\ min^{-1}$)	Uncoated 10^4 P for CO_2 (cm^3 (STP) $s^{-1}\ cm^{-2}\ cmHg^{-1}$)	Coated 10^4 P for CO_2 (cm^3 (STP) $s^{-1}\ cm^{-2}\ cmHg^{-1}$)	Uncoated Ω for CO_2 over CH_4	Coated Ω for CO_2 over CH_4	Polysulfone instrinsic selectivity for CO_2 over CH_4	Surface porosity	Pore radius (Å)	Pore number $(cm)^{-2}$	Distance between pores (Å)
1.0	0.0150	0.0127	2.24	3.38	28.1	1.25×10^{-6}	38.0	2.76×10^6	6.02×10^4
1.33	0.0226	0.0145	1.86	4.04	33.1	1.55×10^{-6}	54.3	1.67×10^6	7.74×10^4
1.67	0.0357	0.0171	1.50	4.28	38.1	2.12×10^{-6}	73.2	1.26×10^6	8.91×10^4
2.0	0.0526	0.0200	1.07	4.53	43.3	3.13×10^{-6}	100.0	1.00×10^6	10.01×10^4

[a] The dope was 40% w/w polysulfone in dimethylformamide and the JS was constant at 1. The thickness of the active layer was 4.31×10^4 Å. On coating, the L_4/r ratio was 0.521. Gas transport was by solution diffusion and Knudsen diffusion

Table 8 Overall permeation data and the effect of jet stretch on fibre structure[a]

JS	Uncoated 10^4 P for CO_2 (cm^3 (STP) $s^{-1}\ cm^{-2}\ cmHg^{-1}$)	Coated 10^4 P for CO_2 (cm^3 (STP) $s^{-1}\ cm^{-2}\ cmHg^{-1}$)	Uncoated Ω for CO_2 over CH_4	Coated Ω for CO_2 over CH_4	Polysulfone instrinsic selectivity for CO_2 over CH_4	Surface porosity	Pore radius (Å)	Pore number (cm^{-2})	Distance between pores (Å)
0.75	0.0153	0.0138	2.35	4.53	27.1	1.06×10^{-6}	40.0	2.10×10^6	6.89×10^4
1.0	0.0187	0.0152	1.85	3.98	28.1	1.42×10^{-6}	46.4	2.10×10^6	6.90×10^4
1.25	0.0246	0.0166	1.33	3.40	27.7	2.03×10^{-6}	59.3	1.84×10^6	7.38×10^4
1.5	0.0309	0.0179	0.89	2.92	20.9	3.00×10^{-6}	78.0	1.57×10^6	7.98×10^4

[a] The dope was 40% w/w polysulfone in dimethylformamide and the DER was constant at 1 $cm^3\ min^{-1}$. The thickness of the active layer was 3.86×10^4 Å. On coating, the L_4/r ratio was 0.521. Gas transport was by solution diffusion and Knudsen diffusion

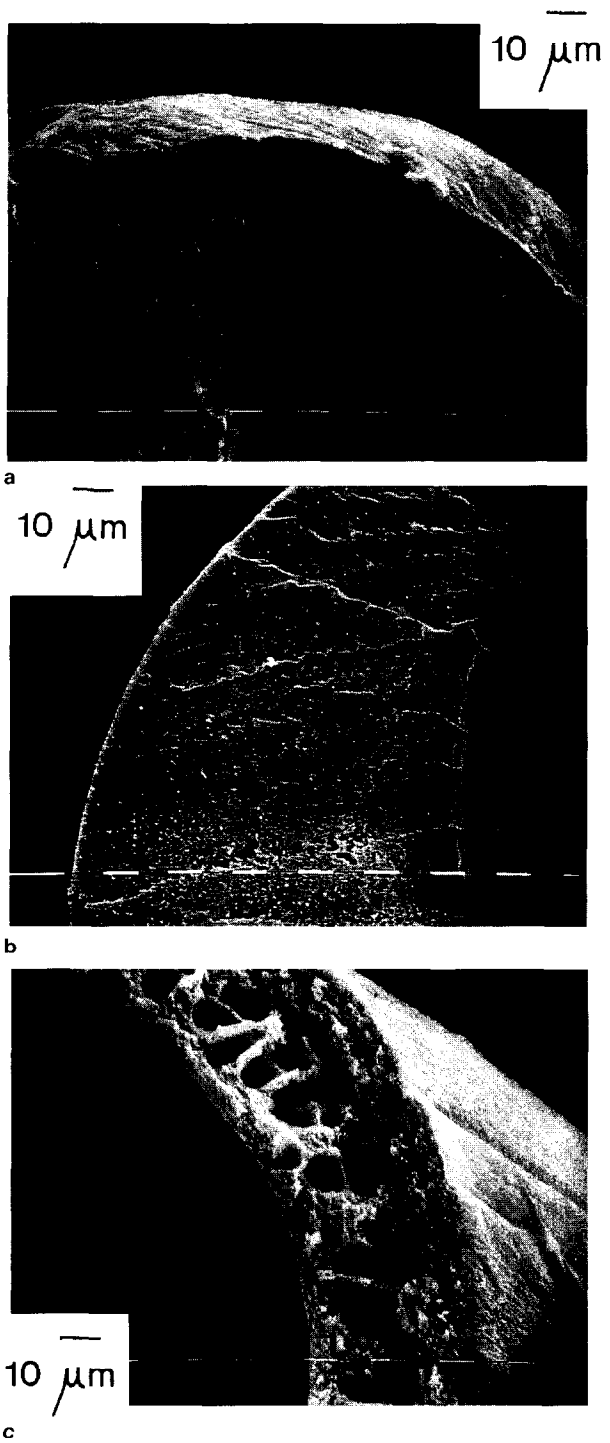

Figure 5 Cross-sections of polysulfone hollow fibres: (a) 40% w/w dope; (b) 30% w/w dope; (c) 20% w/w dope

No surface pores could be visually observed in the skins of any of the fibres by electron microscopy. The maximum magnification achieved was 10000. This indicates that the radius of the pores was generally less than 100 Å, and this value was used at the highest pore size when considering pore size variation. The ratio of L_4 (related to silicone penetration depth) to pore radius r was established at this pore size and assumed constant.

Pore size was found to increase with decreasing polymer concentration in the spinning dope, and values were based on a maximum pore radius of 100 Å. However, for the fibres spun from the 20% w/w and 30% w/w polysulfone dopes, highly permeable in comparison to the 40% w/w spun fibres, an additional pore radius term of 1000 Å was introduced. It should be recognized that a pore size distribution will exist on the membrane surface. Thus, introducing a 1000 Å pore size term as a correction to represent the top end of the Knudsen range in these fibres is not unreasonable. The 1000 Å pores appear only occasionally on the membrane surface (see pore spacings in *Table 4*).

The above working assumptions enabled the resistance modelling to propose sensible structural details which represented the permeation properties of the membranes.

At this point, to increase confidence in the veracity of the modelling, it is worth noting the predicted values of the active layer thickness. It can be seen from *Table 4* that the 40% w/w and 30% w/w spun fibres are predicted to have a similar active layer thickness of around 3–4 μm (10000 Å = 1 μm), much higher than the value of 0.14 μm for the 20% w/w spun fibres. This was confirmed from electron micrographs. *Figures 5a* and *5b* show distinct active layers of appropriate thickness for 40% w/w and 30% w/w fibres. No such discrete layer can be identified in the high voidage 20% w/w fibres, as shown in *Figure 5c*.

Effects of dope concentration (Figures 3 *and* 4 *and* Table 4)

Permeability was found to decrease with increasing dope concentration. Coating obviously reduced permeability and the effect was more marked with fibres spun at low dope concentration. Before coating, the 20% w/w and 30% w/w spun polysulfone fibres exhibited poor selectivities associated with Knudsen diffusion through pores in the active layer ($\Omega_j^i = (M_j/M_i)^{\frac{1}{2}} = 0.603$ for CO_2 against CH_4). In contrast, the 40% w/w spun membranes achieved selectivities of over 2 in favour of CO_2 over CH_4, indicating some solution diffusion transport. After coating, the fibres from all three dope concentrations exhibited solution diffusion selectivities. The 20% w/w and 40% w/w spun fibres showed values between 4 and 5, but the selectivities of the 30% w/w fibres were disappointing, barely reaching 2.

The thickness of the membrane active layer L_1 increases and surface porosity A_P decreases with increasing dope concentration. Coated fibre selectivities decrease with increasing pore area and increasing thickness of the active layer owing to limitations regarding silicone penetration depth. As a result, the product of A_P and L_1 largely controls selectivity; a thin active layer and low pore area correspond to a high selectivity. The 30% w/w spun fibres have both a thick active layer and a large pore area, causing the poor selectivity of these membranes in comparison to those spun from the other two dope concentrations. Permeability increases with increasing pore area and decreasing thickness of the active layer. Permeability decreases with increasing dope concentration because the ratio A_P/L_1 decreases.

The gas transfer modelling also shows that pore size decreases with increasing dope concentration, a result confirmed by water permeation tests and measurements of the variation in permeability with pressure[2].

Coated fibre selectivity values have some degree of sensitivity with regard to pore size since silicone

penetration depth increases with increasing pore size. This finer effect finally accounts for the closeness in the selectivities of the 40% w/w and 20% w/w spun fibres, even though their A_P L_1 values are slightly different.

The 40% w/w spun polysulfone membranes, because of their superior separation characteristics in the uncoated state, were used for studying the effects of dope extrusion rate and jet stretch on fibre performance.

*Effect of dope extrusion rate (*Tables 5 *and* 7*)*

A study of the dope extrusion rate on gas permeation performance provided the most interesting results of this work. Permeability and selectivity increase with increasing dope extrusion rate once the fibres have been coated. Surface pore area increasing with increasing DER would account for the rise in permeability. Taking a simple view, the increase in surface pore area would cause a decrease in selectivity for uncoated and coated fibres alike, since the selectivity of the silicone coating is much lower than that of polysulfone (*Table 2*). The actual rise in selectivity of the coated membranes with increasing DER can be explained in terms of an increase in the selectivity of the polysulfone polymer itself, which is significant enough, even at the generally low coating penetration levels, to cause an increase in the overall selectivity of the coated membrane even though the surface pore area is increased with increasing DER.

The dope extrusion rate results can be related to the rheological behaviour of the spinning dopes under shear. All dopes exhibited shear-thinning behaviour and signs of viscoelasticity[3]. It could be suggested that as the shear rates in the vicinity of the spinneret wall increase owing to increasing DER, the polymer molecules become more aligned. It is this enhanced orientation that may be the cause of the improving selectivity of the polymer with increasing DER. Viscoelastic effects would certainly explain the presence of a highly oriented skin region. Coagulation occurs rapidly on extrusion and thus structure is 'frozen' into the fibre wall before relaxation can take place. Further coagulation of the relaxed core by diffusion results in the differing morphology between skin and core. This is a well-documented phenomenon in textile fibre spinning[16]. This would certainly apply to the inner skin of the hollow fibres where coagulation is instantaneous.

*Effect of jet stretch (*Tables 6 *and* 8*)*

Permeability increases and selectivity decreases with increasing jet stretch ratio for both uncoated and coated fibres. These results can again be explained in terms of structural variations in the membranes as suggested by the gas transfer modelling. As jet stretch increases, both pore area and pore size increase. During the coagulation process as incipient skin formation occurs, elongation of the weak skin will occur. Failure of the thin membrane will take place with a constant exposure of new solution to coagulant until the skin is strong enough to resist deformation. The result is an increase in the area and size of surface pores in the skin. The effect would be predominant on the inner surface.

The most interesting effect from a purely rheological standpoint is that the modelling also indicates a decrease in the selectivity of the solid polymer as jet stretch increases. The elongational viscosity tests carried out on the spinning dopes[2,3] indicated that the fluids were strain thinning. This is generally taken to indicate a progressive fall in entanglement-induced orientation in the polymer solution, which may result in an unfavourable molecular structure, with respect to selectivity, on polymer solidification.

CONCLUSIONS

The modelling work carried out allows fine structural details to be proposed that explain the performance of gas separation hollow fibre membranes. This structural information also relates fibre performance to spinning conditions. The conclusions can be summarized as follows.

1. Dope concentration determines the general morphology of a fibre: the porosity (voidage fraction), thickness of the active layer and order of magnitude of surface porosity (fraction of surface area that is pores).
2. Permeability decreases with increasing dope concentration since the ratio of surface porosity to active layer thickness decreases.
3. Uncoated membrane selectivities are poor because surface porosity levels are sufficiently high ($> 10^{-6}$) to cause pore flow to dominate. Selectivity increases as the product of the active layer thickness and the surface porosity decreases. The lowest coated fibre selectivities occur with the fibres spun from the medium spinning dope concentration because both surface porosity and active layer thickness are high in these membranes.
4. DER and JS are seen to affect solid polymer selectivity, which sets the maximum selectivity that could be achieved by a particular membrane if coating was highly effective or if no surface pores were present. To maximize the potential selectivity of a membrane, a low JS and high DER should be employed. Such a combination achieves the most favourable polymer orientation in the skin region.
5. A minimum active layer thickness is desirable to maximize permeability. A low dope concentration is favourable in this regard.

The structures proposed above do accurately account for fibre performance but further experimental work is necessary to validate their actual existence. Spinning and coating procedures should be improved to increase the range of membrane selectivities. The direct measurement of polymer molecule orientation by spectroscopic techniques is also required to confirm the effects on solid polymer selectivity. Such work is under way and will be reported in a separate paper.

REFERENCES

1 van't Hof, J. A., Reuvers, A. J., Boom, R. M., Rolevink, H. H. M. and Smolders, C. A. *J. Membrane Sci.* 1992, **70**, 17
2 Shilton, S. J. PhD Thesis, University of Strathclyde, 1992
3 Shilton, S. J., Bell, G. and Ferguson, J. *Polymer* 1994, **35**, 5327
4 Henis, J. M. S. and Tripodi, M. K. *Sep. Sci. Technol.* 1980, **15**, 1059
5 Henis, J. M. S. and Tripodi, M. K. *J. Membrane Sci.* 1981, **8**, 233
6 Fouda, A., Chen, Y., Bai, J. and Matsuura, T. *J. Membrane Sci.* 1991, **64**, 263
7 Kirk, A. D. *J. Chem. Educ.* 1967, **44**, 745

8 Barrer, R. M. 'Diffusion in and through Solids', Cambridge University Press, Cambridge, 1951
9 Treybal, R. E. 'Mass-Transfer Operations', 3rd Edn, McGraw-Hill, New York, 1981
10 Chern, R. T., Koros, W. J., Hopfenberg, H. B. and Stannett, V. T. in 'Materials Science of Synthetic Membranes' (Ed. D. R. Lloyd), American Chemical Society, Washington, DC, 1985, p. 25
11 Robb, W. L. *Ann. N.Y. Acad. Sci.* 1967, **146**, 119
12 Present, R. D. and de Béthune, A. J. *Phys. Rev.* 1994, **75**, 1050
13 Dushman, S. 'Scientific Foundations of Vacuum Techniques', 2nd Edn, Wiley, New York, 1962
14 Sourirajan, S. and Agrawal, J. P. in 'Reverse Osmosis and Synthetic Membranes' (Ed. S. Sourirajan), National Research Council of Canada, Ottawa, 1977, p. 527
15 Moore, W. J. 'Physical Chemistry', 5th Edn, Longman, Harlow, 1972
16 Ziabicki, A. 'Fundamentals of Fibre Formation', Wiley, New York, 1976

APPENDIX: VARIABLES AND CONSTANTS

A membrane surface area (cm^2)
A_p fraction of membrane surface area that is pores (surface porosity)
C_D spinning dope concentration (% w/w)
D diffusion coefficient (diffusivity) ($cm^2 s^{-1}$)
d_m molecular diameter (Å)
L length or thickness (Å or μm or cm)
M molecular weight ($g\,mol^{-1}$)
N Avogadro constant
N_p number of pores per unit membrane surface area cm^{-2}
p pressure (bar or cmHg)
Δp pressure difference (bar or cmHg)
$\bar{P}$ permeability coefficient (cm^3(STP) $cm\,s^{-1}$ cm^{-2} $cmHg^{-1}$)
P permeability (cm^3(STP) s^{-1} cm^{-2} $cmHg^{-1}$)
Q flow rate (cm^3(STP) s^{-1} or $mol\,s^{-1}$)
R_0 universal gas constant ($J\,mol^{-1}\,K^{-1}$)
R resistance to gas permeation ($s\,cmHg\,cm^{-3}$ (STP))
r radius of pore (Å)
S solubility coefficient ($mol\,cm^{-3}\,bar^{-1}$)
T temperature (K)
η viscosity ($N\,s\,m^{-2}$)
λ mean free path (Å)
Ω selectivity (P_i/P_j)

APPENDIX: CLASSIFICATIONS AND SUBSCRIPTS

C coated
U uncoated
1 membrane active layer
2 pore
3 silicone coating layer
4 silicone pore overlay plus penetration
i component i (CO_2)
j component j (CH_4)
f feed
p permeate